Scientific
Research
Publishing

Thermodynamic Study and Exergetic Analysis of the Integrated SOFC-GT-Kalina Power Cycle

Hongbin Zhao[1,2*], Xuan Hou[1,2], Qian Yang[1,2]

[1]College of Machinery and Transportation Engineering, China University of Petroleum, Beijing, China
[2]Beijing Key Laboratory of Process Fluid Filtration and Separation, Beijing, China
Email: *hbzhao@cup.edu.cn

Abstract

In this paper the SOFC-GT-Kalina (solid oxide fuel cell, gas turbine, and Kalina cycle) integrated system is proposed. The system uses Kalina cycle as the bottoming cycle to recovery the waste heat from the gas turbine to generate power. Kalina cycle uses ammonia-water mixture as the work fluid which has sliding-temperature boiling characteristics. By comparing with the SOFC-GT-ST (solid oxide fuel cell, gas turbine, and steam turbine cycle) system as the reference system, the systems are simulated by Aspen Plus through analyzing the overall system performance. Electrical and exergy efficiency of the proposed system are 74.41% and 71.93%, and electrical and exergy efficiency of the reference system are 71.45% and 69.07%, proving the superiority of Kalina cycle for waste heat recovery. In addition, the exergy losses of each component are studied, and the detail performance analysis of the proposed system is presented, consisting of thermal analysis, exergy analysis and EUD (Energy-utilization diagram) analysis, which intuitively disclosed the causes of exergy loss. Additionally, it was revealed that there exists an optimal current density at 350 mA/cm^2 for power and power density.

Keywords

1. Introduction

Now, distributed power systems are more and more popular, because it can reduce losses during transmission and distribution of power; in addition, it can flexibly adjust to user demand change. As a kind of modular power generation device, SOFC is suitable for distributed power generation. SOFC has a lot of ad-

vantages, for example it can directly convert chemical energy of fuel into electricity with little pollution, which is different from the traditional power generation mode being limited by Carnot cycle efficiency. In addition, because of its high operating temperature, its high-temperature exhaust gas (about 650°C - 1000°C) can be used to drive combined cycle [1] [2] [3]. Hybrid power generation system can make full use of exhaust gas and improve the total energy utilization. In recent years, along with the technical progress of SOFC, integrated cycle driven by SOFC also gets rapid development.

The concept of SOFC-GT integrated system has been proposed for many years. Ali Volkan Akkaya etc. [4] proposed a SOFC-GT CHP system and used HRSG for waste heat recovery; exergy analysis is carried out based on the developed model to analyze the system performance. Andrew S. etc. adopted a FORTRAN-based dynamic simulation model of an SOFC-GT system to analyze the system performance [5], and then made comparative analysis of SOFC-GT freight locomotive fueled by natural gas and diesel with inboard reformation. The results proved that SOFC-GT system can provide a 54% savings in CO_2 for operation on natural gas. The authors [6] proposed three different SOFC hybrid power systems with zero-CO_2 emission. Paper [7] presented a full and partial load exergy analysis of a hybrid SOFC-GT power plant, and paid special attention to calculate the SOFC over-potentials. The study also showed energy and exergy flows through all its components and thermodynamic properties at each key-point. Ehsan Baniasadi [8] proposed an integrated heat and power (CHP) system for vehicular applications and used ammonia fuel in SOFC to produce hydrogen and nitrogen at the anode. The performance of the portable SOFC system was studied in a wide range of the cell's average current density and fuel utilization ratio. Its exergy efficiency is calculated to be 60% - 90% as a function of current density, whereas energy efficiency varies between 60% and 40% respectively. The paper [9] proposed an integrated gasification and SOFC system with a GT and ST to use heat recovery of the GT exhaust. The study [10] presented the integration of direct ammonia SOFC with a GT in a combined CCHP cycle system. The results revealed that the SOFC-H integrated system can offer better performance than that with the SOFC-O option. The study [11] provided the energy and exergy performance analysis of a SOFC-GT-ST combined cycle power plant; this study also used additional fuel burning in the combustion chamber to increase net power of GT and ST. The results showed additional fuel can improve GT and ST power, but reduce the overall system efficiency. The paper [12] presented exergy analysis of a hybrid SOFC-GT system in comparison with retrofitted system with steam injection. GT exhaust gas was used to generate steam, and then injects team into ST. Results showed that this way can bring 17.87% and 12.31% increase of exergy output and the thermal efficiency, and the exergy and thermal efficiency of the integrated cycle can get as high as 57.9% - 60.6% respectively at the optimum compression ratio [13]. The study used SOFC-GT to drive Stirling engine to provide heat and power, and the results showed that it can deliver electricity at a cost that is competitive with the

corresponding renewable systems of the same size [14]. Through system integration, many researchers constantly put forward various efficient thermal cycles and carry out related research. A novel integrated system [15], including solid oxide fuel cell (SOFC), steam cycle with liquefied natural gas (LNG) vaporization and so on, is configured and analyzed showing that SOFC operating parameter shave a significant effect on the overall process performance. The integration of SOFC with intercooled gasturbine cycle is reported [16], and its performance has been optimized by entropy generation minimization considering other factors such as recirculation ratio, mass of fuel and TIT (turbine inlet temperature). By introducing (retrofitting) solid oxide fuel cells (SOFCs) and CO_2 capture in existing IGCC power plants utilizing high percentage(up to 70%) biomass co-gasification [17] was proposed and various thermodynamic aspects have been studied to retrofit SOFCs in IGCC systems. From the former studies we know these cycles can use the exhaust heat to a certain degree, but not perfect. This is due to that at the evaporation process, evaporation temperature of pure working fluid is constant, while the temperature of the heat source is a variable, temperature match is not good which can lead great irreversible loss.

Kalina cycle is put forward to improve Rankine cycle; it can be used as bottom cycle to recover the waste heat from the gas turbine to generate power. Kalina cycle uses ammonia-water mixture as the working fluid which has sliding-temperature boiling characteristics. On the other hand, due to the boiling point of ammonia is much lower than water, it can be easily gasified at low temperature [18] [19] [20], so Kalina cycle has obvious advantage when using low temperature waste heat, which has been used as bottom cycle in many studies, such as solar energy, GT-Modular Helium Reactor, internal combustion engine, coal fired steam power plant, geothermal energy and so on. The study [21] investigated a Kalina cycle using low-temperature heat sources to produce power. The heat source is provided from flat solar collectors. For given conditions, there exists an optimum range of vapor mass fractions and operating pressures. The study [22] used the solar-boosted system with an auxiliary super heater to drive Kalina cycle and analyzed its performance. Paper [23] employed organic Rankine cycle (ORC) and Kalina cycle for heat recovery from the GT-Modular Helium Reactor and made comparison of the performances. Although the simple configuration of ORC can be accounted as its advantage, the KC may have better performance from the second law perspective [24]. KC and ORC cycle was conducted in order to analyze energy saving of the sensible exhaust waste heat recovery under various internal combustion engine (ICE) working conditions [25]. The extremely high turbine expansion ratio requires a complex multi-stage turbine design and large turbine dimensions for the bottoming transitional ORC using Alkanes-based working fluid [26]. Studies [27] on technology and economy analysis of the KC by Lv reveal the essence and direction of improvement. Zhang [28] analyzed the influence of key parameters on the performance of KC. The paper [29] provided a computer simulation of KC coupled with a coal fired steam power plant, and also studied the effect of main parameters such as am-

monia mass fraction, AT inlet pressure on the system performance. The paper [30] made energy and exergy analysis and parameter design optimization of the KCS-11 solar system with an auxiliary super heater. The power generated by each major equipment and the main system exergy losses are calculated in this paper. The study [31] used KCS-34 to generate electricity from geothermal resources with low and medium enthalpy, and adopted life-cycle-cost concepts to study the system, taking Kalina system efficiency and economy into account as the objective functions, a multi-objective optimization design is conducted. The results showed that there was an optimum ammonia concentration which matched with each optimal performance. However, Kalina cycle also has some disadvantages, Dipippo [32] considered that the difference in efficiency between the Kalina circulatory system and the ORC circulatory system is 3%, but the structure of Kalina cycle is more complicated. Bombarda [33] compares the thermodynamic properties of the Kalina and ORC cycle, argues that the stresses in the Kalina circulatory system are too high and not conducive to the stability of the system. Fu [34] believes that ORC and Kalina cycle have their own suitable heat source temperature range, and the high efficiency of the Kalina loop system is at the cost of high pressure.

As can be seen, in Kalina cycle temperature match can be improved, which can improve the heat exchange process. Previous studies have combined the first law of thermodynamics, the second law of thermodynamics, parameter optimization, system economics analysis, artificial neural network analysis, EES engineering equation solver, genetic algorithm, etc., having guiding significance for further study. But little research has been found to use Kalina cycle to recover SOFC-GT waste heat as well as do comprehensive performance analysis of the SOFC-GT-Kalina system. The objective of the study is to present a thermodynamic analysis of SOFC-GT-Kalina cycle based on the first and second law of thermodynamics, as well as the comparison with SOFC-GT-ST system, at the same time, using EUD analysis method to disclose the nature of exergy loss.

2. System Descriptions

2.1. The Process of the Combined Cycle

Figure 1 illustrates the SOFC-GT-Kalina integrated system proposed, and Figure 2 shows the reference SOFC-GT-ST system flow chart. We can see in the figures, after being compressed by Fuel compressor and reformed in Reformer, the flue gas (3) is fed to anode of SOFC stack. After being compressed by Air compressor and reheated by waste heat from GT exhaust gas (14), air (8) is fed to SOFC cathode. Inside the SOFC cell stack, oxygen is dissociated into oxygen ions at the cathode surface, which then get to the anode through the electrolyte and occurs electrochemical reaction with fuel at anode. Part of the SOFC exhaust gas (5) recycles to the fuel pre-reforming unit to supply water and heat for the endothermic steam reforming. The excess air (11) and unreacted fuel (6) out of SOFC combust completely in Afterburner, then the high temperature and high
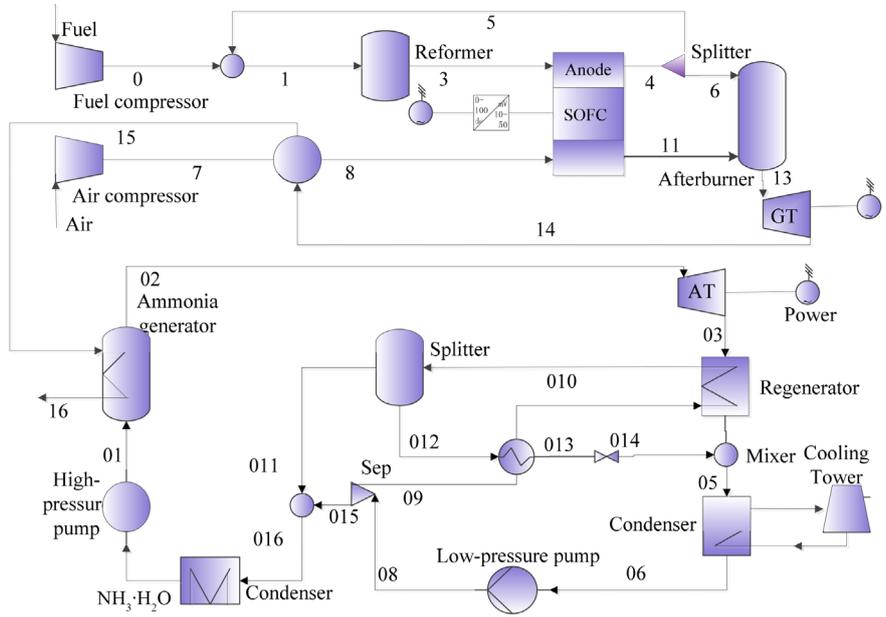
Figure 1. The proposed SOFC-GT-Kalina system flow chart.
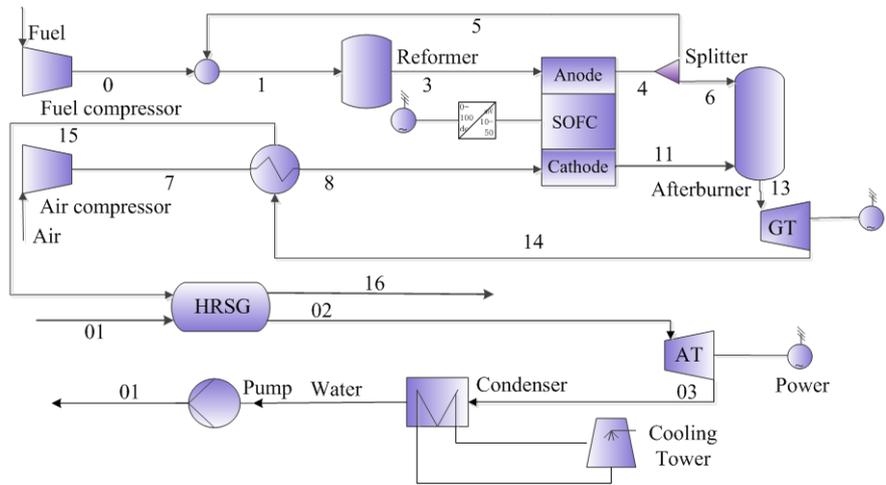
Figure 2. The reference SOFC-GT-ST system.

pressure gas (13) flow into GT and generate electricity there. The exhaust gas from GT (14) is sequentially used to preheat the air, and then (15) flow into Kalina cycle or Rankine cycle for further heat recovery, in this way to realize the cascade utilization of energy and improve the efficiency of the overall system.

The basic Kalina cycle (KC) is similar with Rankine cycle (RC), mainly consisting of HRSG, turbine and condenser, the main difference is that Kalina cycle uses a distillation subsystem to solve the condensation problem of ammonia-water mixture.

In the proposed system, KC uses ammonia-water mixture as working fluid. The saturated working fluid (NH_3/H_2O) is boosted through high-pressure pump (01), then turns into superheated gas (02) in an ammonia generator which can

generate power in AT. Exhaust steam (03) from AT is cooled by regenerator, and mixes with rich aqueous solution (014) from the bottom of the distillation to form the basic solution (05), then condensed completely to saturated liquid (06) through the low-pressure condenser and boosted through low-pressure pump (08). Stream (08) flows into the Sep, a surge (09) after being heated by regenerator (010) flows into the distillation, then separated into rich ammonia solution (011) and rich aqueous solution (012); Another surge mixes with the rich ammonia solution (011) to form working solution (016), then through high-pressure condenser is condensed into saturated working solution ($NH_3 \cdot H_2O$), in this way to complete the cycle.

In the reference system, RC uses water as working fluid, and produces high pressure (01) and high temperature steam (02) which can generate power in ST.

2.2. Basic Parameters and General Assumptions

The parameters and structural size involved in the process simulationis according to the tubular designed by Siemens-Westinghouse, as shown in Table 1 and Table 2 [35].

We also need to make some assumptions for calculation as follows:

1) Considering the velocity of the fluid flow through the relevant components, heat losses from system to environment are negligible; 2) Temperature and pressure inside the battery are almost uniform, all the battery cells within the stack are in the same state; 3) Due to the high temperature and low pressure, the reaction gas can be regard as ideal compressible gas; 4) Because of good sealing, the mass loss of each component is ignored; 5) The dynamic performance of the system is not considered in this paper, all reactions are in equilibrium state, and SOFC works under steady-state operation; 6) The process is relatively short through the cell stack, the mass and pressure loss in it are negligible. These assumptions may have certain error effect on the absolute values of the calculation results, but do not affect the understanding of the system law.

3. The Mathematical Model

To evaluate the performance of the system, the first law and the second law method can be used. For the first law perspective, performance indicators mainly include: current density, voltage, power, electrical efficiency and power density. For the second law perspective, performance indicators mainly include: exergy losses and exergy efficiency. The formulas in this paper are based on the classical formulas in the literature [36].

Table 1. The size parameter of SOFC.

Parameter	Size
Battery length	150 cm
Battery outer diameter	2.2 cm
Cell reaction area	260 cm^2

Table 2. The main parameters of SOFC-GT cycle.

Parameter	Value	Parameter	Value
Fuel inlet temperature/°C	25	Air inlet temperature/°C	25
Fuel inlet pressure/bar	1	Air inlet pressure/bar	1
Steam/carbon ratio	2.5	DC-AC conversion efficiency/%	98
SOFC heat loss/%	2	SOFC operating pressure/bar	10
Compressor polytropic efficiency/%	85	Turbine polytropic efficiency/%	85
Compressor mechanical efficiency/%	99	Turbine mechanical efficiency/%	99

3.1. The Current Density Model of SOFC

The current density model of SOFC can be defined as Equation (1):

$$I = \frac{n \times F \times 4 q_{CH_4}}{N_{cell} \times A_{cell}} \tag{1}$$

where: n—Electrons number transferred of each Oxygen atom in the electrochemical reaction, taking 2; F—Faraday constant, 96,485 C/mol; q_{CH_4}—methane molar flow rate, mol/s; N_{cell}—number of cells; A_{cell}—single-cell area, m^2.

3.2. The Voltage Model of SOFC

Firstly, select the reference voltage, and then by calculating the influence of pressure, temperature, gas pressure on voltage at other non-reference state to calculate voltage value.

$$\Delta V_p \, (\text{mV}) = C_1 \times \log \left(p / p_{ref} \right) \tag{2}$$

where: $\Delta V_p \, (mV)$—The influence of operating pressure on the voltage, mV; $C_1 = 76$; p—The SOFC operating pressure, bar; P_{ref}—Reference pressure, 1 bar.

$$\Delta V_T \, (\text{mV}) = K \times \left(T - T_{ref} \right) \times I \tag{3}$$

where: V_T—The operating temperature on voltage, mV; $K = 8$; T—The SOFC operating temperature, °C; P_{ref}— Reference temperature, 1000°C.

$$\Delta V_{an} \, (\text{mV}) = 172 \times \log \left(p_{H_2} / p_{H_2O} \right) / \left(p_{H_2} / p_{H_2O} \right)_{ref} \tag{4}$$

where: ΔV_{an}—The influence of hydrogen and water vapor partial pressure on the voltage, mV; p_{H_2} / p_{H_2O}—Pressure ratio of hydrogen and water vapor; $\left(p_{H_2} / p_{H_2O} \right)_{ref}$—Pressure ratio of hydrogen and water vapor at reference condition, taking 0.15.

$$\Delta V_{cat} \, (\text{mV}) = 92 \times \log \left(p_{O_2} / \left(p_{O_2} \right)_{ref} \right) \tag{5}$$

where: ΔV_{cat}—The influence of the oxygen partial pressure in cathode on voltage, mV; p_{O_2}—The average oxygen partial pressure in cathode, bar; $\left(p_{O_2} \right)_{ref}$—Oxygen partial pressure at reference condition, taking 0.164.

In summary, the SOFC voltage can be obtained as the Equation (6) below:

$$V_{SOFC} = \left(V_{ref} + \Delta V_p + \Delta V_T + \Delta V_{cat} + \Delta V_{an}\right)\Big/1000 \tag{6}$$

where: V_{SOFC} —The *SOFC* voltage, *V*.

3.3. Thermal Performance Evaluation Index

When using the first law of thermodynamic to evaluate the combined system, we use *SOFC* power, *SOFC* electrical efficiency, electrical efficiency of the overall system, total power etc. as the evaluation indexes.

Since the electrochemical reaction occurs in the cell stack, and the whole system is assumed to be adiabatic, therefore the total power generation of the fuel cell can be shown as the Equation (7):

$$W_{DC} = V_{SOFC} \times I \tag{7}$$

SOFC electrical efficiency can be defined as Equation (8):

$$\eta_{SOFC} = \frac{W_{DC} \times 0.92}{m_f \times LHV_f} \times 100\% \tag{8}$$

where: 0.92—DC/AC conversion efficiency; LHV_f—Low heat value of fuel, kJ/kg.

The electrical efficiency of proposed and reference system can be defined as Equation (9) and (10):

$$\eta_{pro-s} = \left(W_{SOFC} + W_{GT} + W_{AT} - W_{AC} - W_{FC} - W_{LP} - W_{HP}\right)\Big/\left(m_f \times LHV_f\right) \times 100\% \tag{9}$$

$$\eta_{ref-s} = \left(W_{SOFC} + W_{GT} + W_{ST} - W_{AC} - W_{FC} - W_{PUMP}\right)\Big/\left(m_f \times LHV_f\right) \times 100\% \tag{10}$$

3.4. Exergy Analysis Evaluation Index

With doing the second law of thermodynamics analysis, exergy efficiency and exergy loss is always used to evaluate the thermodynamic perfection degree of devices. For the total system, as Equation (11):

$$\sum_k \left(E_{in}\right)_k = \sum_j \left(E_{out}\right)_j + \sum_i W_i + I \quad \eta_{ex} = Ex_{gain}\big/Ex_{pay} \le 100\% \tag{11}$$

where: E_{in}—Input exergy, E_{out}—Output exergy, W_i—Power, I—System exergy loss.

Exergy efficiency and exergy loss for compressor, turbine, heat exchanger and SOFC are shown as Equations (12)-(15):

$$\eta_{ex,C} = Ex_{gain}\big/Ex_{pay} = \left(Ex_{out} - Ex_{in}\right)\big/W_C \quad Ex_{L,C} = Ex_{in} - Ex_{out} + W_C \tag{12}$$

$$\eta_{ex,T} = W_{net}\big/\left(Ex_{in} - Ex_{out}\right) \quad Ex_{L,T} = Ex_{in} - Ex_{out} - W_{net} \tag{13}$$

$$\eta_{ex,HE} = \frac{Ex_{gain}}{Ex_{pay}} = \frac{\text{exergy gained by cold fluid}}{\text{exergy paied by hot fluid}} \quad Ex_{L,HE} = \sum Ex_{in} - \sum Ex_{out} \tag{14}$$

$$Ex_{an,in} + Ex_{ca,in} = Ex_{an,out} + Ex_{ca,out} + W_{SOFC} + Ex_{L,SOFC} \tag{15}$$

4. Results and Analysis

4.1. Performance Analysis of Specific Condition

In this paper, we use Aspen Plus for simulation, and select more reasonable basic

parameters for a specific condition analysis. In this paper, the simulation fuel of the SOFC inlet includes 97% of CH_4 and 3% of N_2. GT exhaust gas temperature is 680.2 K. The ammonia-water mass concentration is 70% and AT pressure ratio is 24 as the specific conditions. By Simulation we can get thermodynamic parameters at each working point of the proposed system in Table 3.

For comparing the two systems, firstly we need to specify the external heat source and cooling water conditions which are exactly the same. When keeping former SOFC-GT under the same operating conditions, make comparison between the performances of the two systems, in order to verify Kalina superiority. Table 4 is performance indexes comparison between proposed system and reference system, it can be seen from the results that using Kalina cycle to recovery waste heat can obvious improve the thermodynamic properties than Rankine cycle. The total electrical efficiency is 2.96% higher and the total exergy efficiency is 2.86% higher, indicating Kalina cycle performance has been significantly improved.

Figure 3 shows the exergy destruction of each components. As can be seen from the figure, the largest exergy destruction occurs in the SOFC being 343.74 kW, accounting for 42.78% of all energy losses. Then follow by the after-burner

Table 3. Results of simulation for SOFC-GT-Kalina system.

No.	Temperature [K]	Pressure [bar]	Mass flow [kg/s]	LHV [kJ/kg]
FUEL	298.1	1	0.059	47,466.59
0	520.3	10	0.059	47,466.59
1	1019.5	10	0.443	8219.40
6	1173.2	10	0.25	2165.22
AIR	298.1	1	1.523	0.00
7	635.9	10	1.523	0.00
8	925.7	10	1.523	0.00
11	1173.2	10	1.332	0.00
13	1435.7	10	1.582	0.02
14	935.7	1	1.582	0.02
15	680.2	1	1.582	0.02
16	343.1	1	1.582	0.02
$NH_3 \cdot H_2O$	298.15	9	0.242	13,022.53
01	299.10	72	0.242	13,022.53
02	649.10	72	0.242	13,022.53
03	373.70	3	0.242	13,022.53
06	291.10	3	0.369	9554.07
010	370.77	9	0.258	9554.07
011	370.78	9	0.132	15,939.16
012	370.78	9	0.127	2921.50
016	337.98	9	0.242	13,022.03

Table 4. Performance comparison between the proposed and reference systems.

Parameter	Value	Parameter	Value
SOFC current density/A/m^2	2393.9	SOFC operating voltage/V	0.714
SOFC operating temperature/K	1173	SOFC electrical power/kW	1510.15
After burner temperature/K	1273	SOFC electrical efficiency/%	53.74
Fuel compressor power/kW	33.03	GT power/kW	1016.41
Air compressor power/kW	537.06	AT power/kW	139.88
High-pressure pump power/kW	2.61	ST power/kW	105.34
Low-pressure pump power/kW	0.34	Input exergy/kW	2908.36
Total net power of the proposed system/kW	2092.076	Total net power of the reference system/kW	2008.858
Total electrical efficiency of the proposed system/%	74.414	Total electrical efficiency of the reference system/%	71.454
Total exergy efficiency of the proposed system/%	71.933	Total exergy efficiency of the reference system/%	69.072
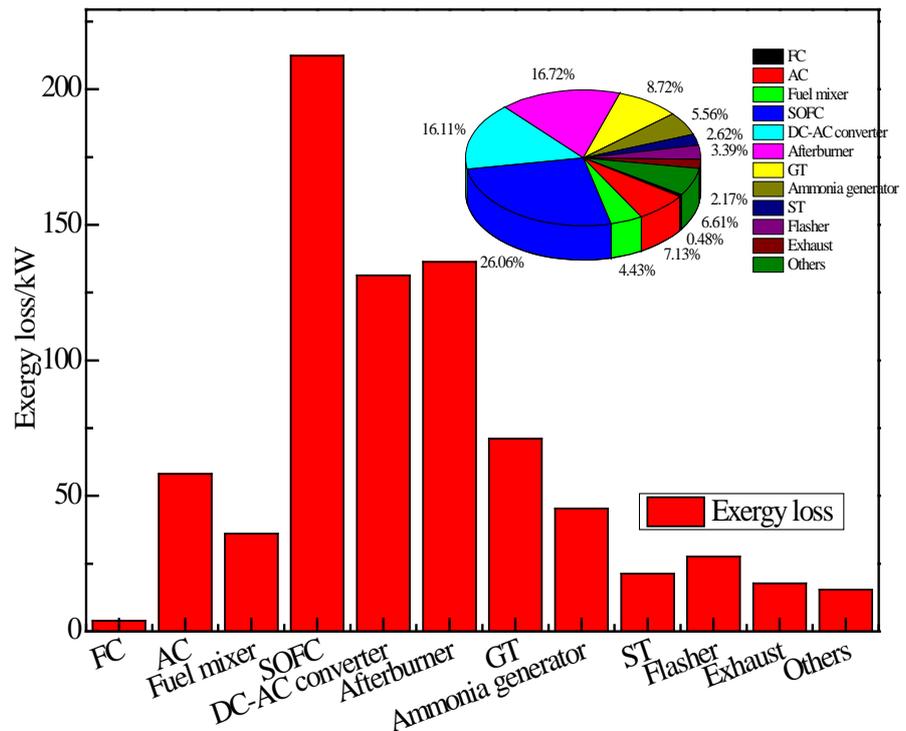
Figure 3. Exergy destruction of each component in SOFC-GT-Kalina system.

for 136.26 kW, accounting for 16.72%. Gas turbine exergy loss is 71.07 kW, accounting for 8.72%. Energy loss of ammonia generator is 45.34 kW, accounting for 5.56%, and its exergy efficiency can get 80.9%. As for the small temperature difference, it can reduce the damage caused by heat transfer irreversible. Exhaust gas temperature is controlled at 70˚C, its energy destruction is 17.71 kW, accounted for a small proportion. We can see from the result that a lot of measures can be taken to increase system utilization, SOFC's exergy loss can be reduced by

improving the interior materials or selecting the appropriate operating temperature and operating pressure; The maximum loss of combustor is mainly combustion irreversible loss, it can be reduced by choosing a suitable air, fuel flow; Energy loss of heat exchanger also have great controllability, selecting an appropriate heat exchanger temperature difference can reduce its exergy loss; To take full advantage of exhaust heat in the exhaust gas, when ensuring the temperature above the dew point, we can use it to a situation temperature as low as possible, thus reducing the exergy taken away by exhaust gas.

By energy analysis we can find out the weaknesses in the system energy use, system performance can be optimized by improving the performance of SOFC, optimizing heat exchanger arrangement, minimizing the temperature difference.

4.2. Influence of Compressor Pressure Ratio on the Integrated System

Figure 4(a) and Figure 4(b) respectively shows the effects of compressor pressure ratio on the exergy destruction in each component.

As can be seen from Figure 4(a), when the fuel flow and fuel utilization remains constant, as the compressor pressure ratio increases, the exergy destruction of SOFC decreases, this is due to SOFC operating pressure increases as the pressure ratio increases, it helps the electrochemical reaction react more completely and irreversible loss of reaction reduce. When the compressor pressure ratio increases from 4 to 10, SOFC exergy destruction decreases from 385.95 kW to 350.57 kW; After-burner exergy destruction changes little with the pressure ratio, which is due to its exergy loss is mainly combustion irreversible losses, this is less affected by pressure change. The exergy destruction of AC and GT increases as the pressure rises, but the trend is more and more slowly, because the entropy change increases with the pressure. FC exergy destruction value is quite small, since the fuel flow is relatively small. Exergy destruction of fuel mixer has reduced small amplitude, but not obvious, indicating that the mixing process has little exergy destruction.

We can also see from Figure 4(a) that the largest exergy destruction occurs in SOFC, then after-burner, ammonia gas generator and GT, and the ammonia flow in Kalina cycle is very small, the pump power and pump exergy destruction is small and can be ignored; As the compressor pressure ratio increases, the exergy destruction of ammonia generator decreases, this is due to as the pressure ratio increases, the temperature of GT exhaust gas decreases, temperature difference is smaller; AT exergy destruction decreases as pressure ratio increasing, but more and more slower.

Figure 5(a) shows the effect of pressure ratio on system performance, and Figure 5(b) shows the effect of pressure ratio on exergy efficiency of main components. As can be seen from Figure 5(a), when the pressure ratio changes from 5 to 10, the overall system electrical efficiency and exergy efficiency both increase, the overall system electrical efficiency changes from 70.05% to 71.98%, exergy efficiency changes from 72.46% to 74.46% which is a little higher than
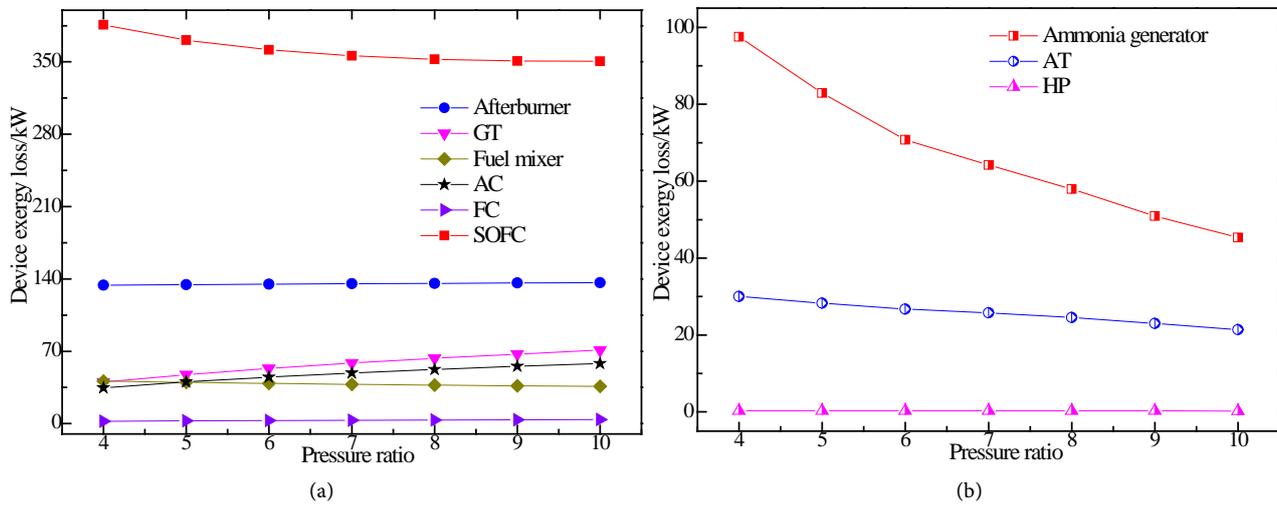
Figure 4. Effects of compressor pressure ratio on the energy destruction in each component.
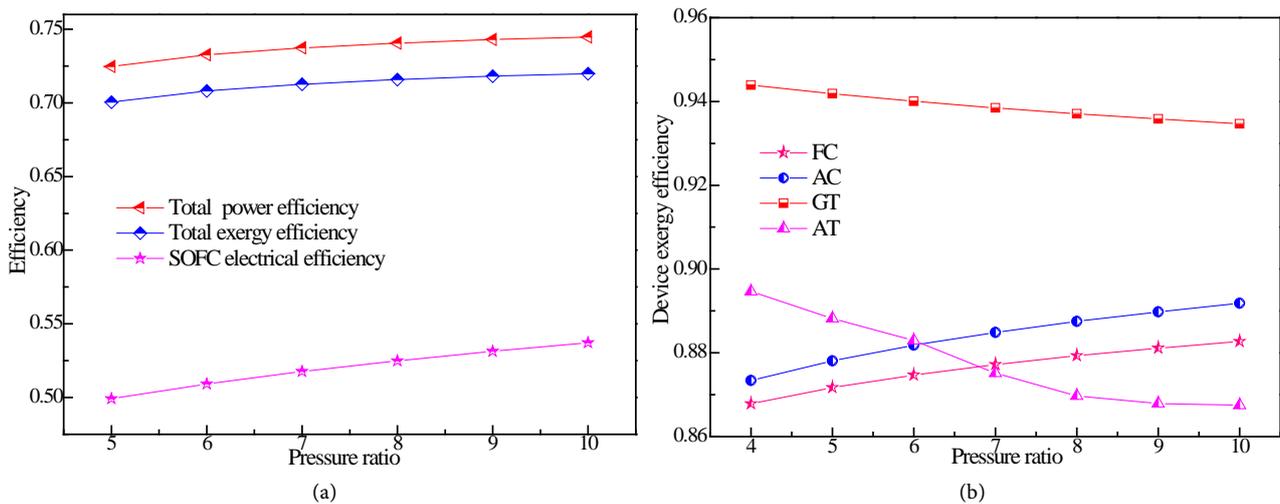
Figure 5. Effects of compressor pressure ratio on the efficiency of system and each component.

electrical efficiency. Electrical efficiency of SOFC changes from 49.92% to 53.715%; as can be seen from **Figure 5(b)**, the exergy efficiency of GT and AT reduces with pressure ratio increasing, exergy efficiency of compressor increases with pressure ratio increasing.

4.3. Influence of Current Density on the Integrated System

Figure 6 shows the influence of current density on system performance. As can be seen, with the increase of current density, SOFC voltage and efficiency both reduce, the AC power and power density both increase and reach a peak at 350 mA/cm² and then decrease. SOFC efficiency decreases mainly because of power increasing (AC and FC) and energy input caused by increasing fuel and air flow rate. We generally expect to make SOFC run at the left of peak, at the same time trade-off between power, efficiency, voltage. There exists an optimal current density at 350 mA/cm².
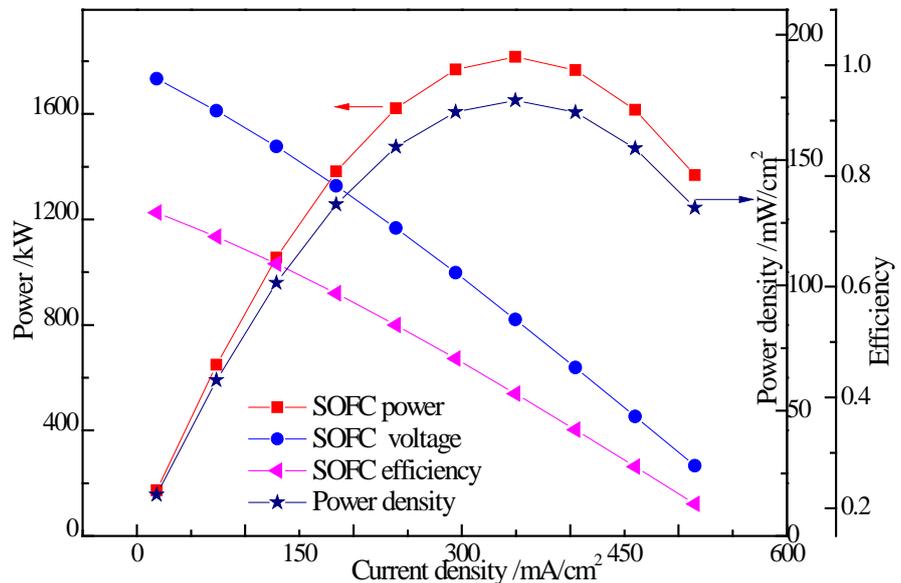
Figure 6. Influence of current density on the performance of the system.

4.4. Influence of Air Mass Flow on the Integrated System

Figure 7 is the influence of air flow on system performance when the air-fuel ratio remains constant. As can be seen from the figure, with the increase of air flow, compressors power consumption increase. SOFC power and SOFC-GT combined cycle power increase slowly at first with air flow, but when the air flow is larger than 180 kmol/h, the power remained almost flat. SOFC efficiency tends to increase within the range of air flow 120 - 200 kmol/h, but the trend is more and more slowly. So the air flow is not the bigger the better when the air-fuel ratio remains constant.

4.5. Influence of ST Inlet Pressure and Ammonia Concentration on the System

Figure 8(a) and **Figure 8(b)** show the impact of AT inlet pressure and ammonia concentration on the energy destruction of ammonia steam generator and ammonia steam turbine respectively.

As can be seen from **Figure 8(a)**, when ammonia concentration keeps constant, the exergy destruction of ammonia generator decreases with the turbine inlet pressure increasing, this is due to as a heat exchanger, higher pressure can bring more benefit for its performance; As can be seen from **Figure 8(b)**, when the ammonia concentration keeps constant, the exergy destruction of AT increases with the turbine inlet pressure increasing, but the trend is more and more slow, this is due to the increasing pressure can lead to an increasing of enthalpy drop between import and export of AT; can also see that keeping turbine inlet pressure constant, AT energy destruction increases with the increasing of ammonia concentration, and the larger the turbine inlet pressure is, the influence is more obvious.
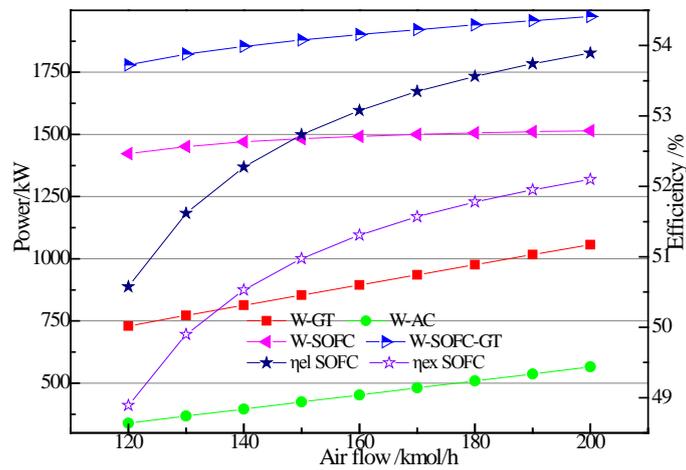
Figure 7. Influence of air mass flow on the performance of the system.
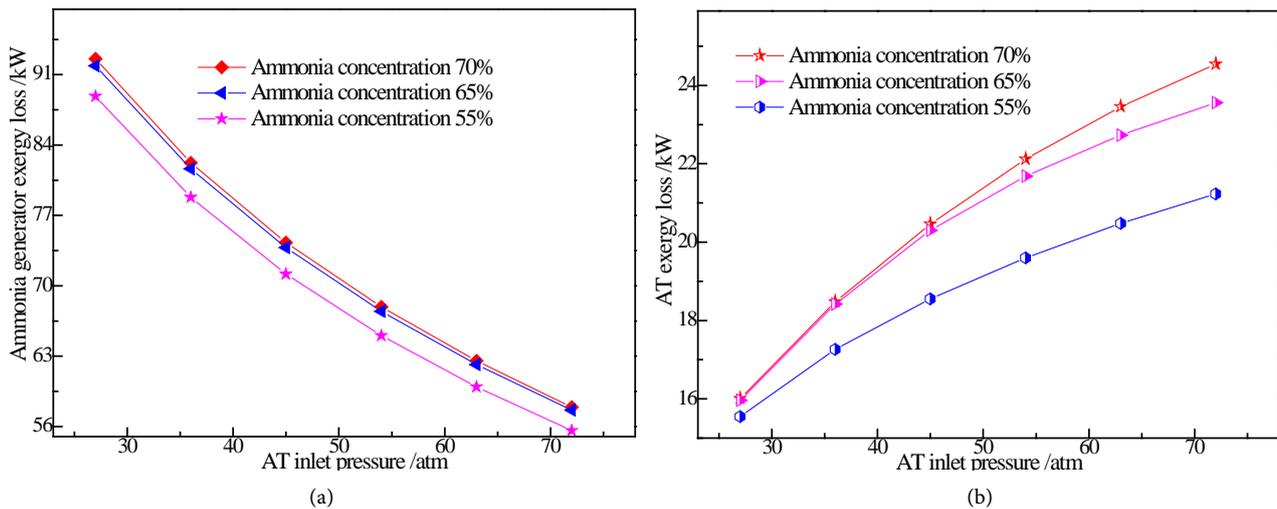
Figure 8. Influence of AT inlet pressure and ammonia concentration on the exergy destruction of main components.

4.6. Influence of Condensation Temperature on the System

In the Kalina cycle when the cooling tower is used as cold source, condensation temperature is greatly affected by ambient temperature. So it's necessary to study the impact of condensation temperature on system performance.

4.6.1. Influence of Condensation Temperature on Thedew and Bubble Temperature

Kalina cycle uses the binary mixture NH_3/H_2O as working fluid which has the characteristics of change temperature in evaporation. At ambient pressure conditions the boiling point of NH_3 is 240 K, and the boiling point of H_2O is 373.34 K, while in the evaporation process, the mixture concentration decreases which can lead to an increasing of the boiling point. Since the Kalina cycle is operating at higher pressures, as basis for calculation, the thermo-physical properties of NH_3/H_2O at higher pressures and temperatures are required. We refer to the ASPEN PLUS simulation results in our calculation. Ammonia mixture should be

fully condensed into a liquid before entering the solution pump, when the condensing pressure is determined, the bubble point and dew point of different concentrations ammonia at condensing pressure is required in order to guide us to determine the condensed water temperature, as shown in Figure 9.

4.6.2. Influence of Condensation Temperature on the AT Outlet Pressure and Kalina Thermal Efficiency

Figure 10(a) shows the impact of condensation temperature on the AT outlet pressure. As can be seen from the figure, when the ammonia concentration is constant, the AT outlet pressure increases with increasing of condensation temperature. When keeping the condensation temperature constant, the AT outlet pressure increases with increasing of ammonia concentration. Also can be seen, the relationship between the outlet pressure and condensation temperature is non-linear, and higher condensation temperature leads to greater pressure difference. We can see, when the condensation temperature is 5˚C, the pressure difference is 1.4 atm, when the condensation temperature is 30˚C, the pressure difference is 3.5 atm.

Figure 10(b) shows the impact of condensation temperature on Kalina efficiency. As can be seen from the figure, Kalina efficiency reduces with the increasing of condensation temperature. This is due to condensation temperature increasing leads to the turbine outlet pressure increase, when turbine inlet pressure keeps constant, its pressure difference decreases, this can further lead to turbine power reduction, reducing efficiency. When the condensation temperature is constant, Kalina efficiency decreases with increasing of ammonia concentration, this is because the higher concentration leads to a greater turbine outlet pressure.

4.7. EUD Analysis of the System

In order to reveal the internal phenomena of the main processes of the proposed system, EUD method which was proposed by Ishida, was adopted in this study.
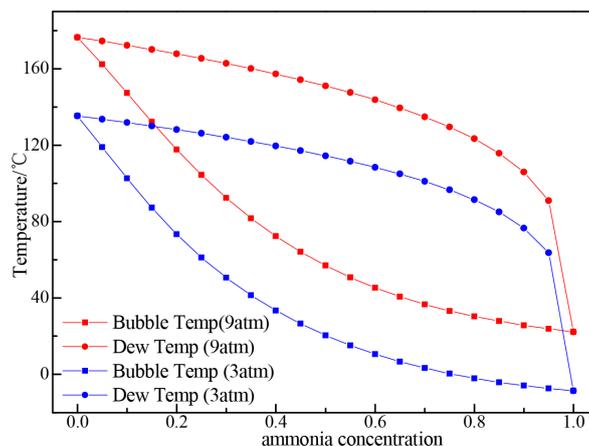
Figure 9. Influence of ammonia concentration on the dew and bubble temperature.
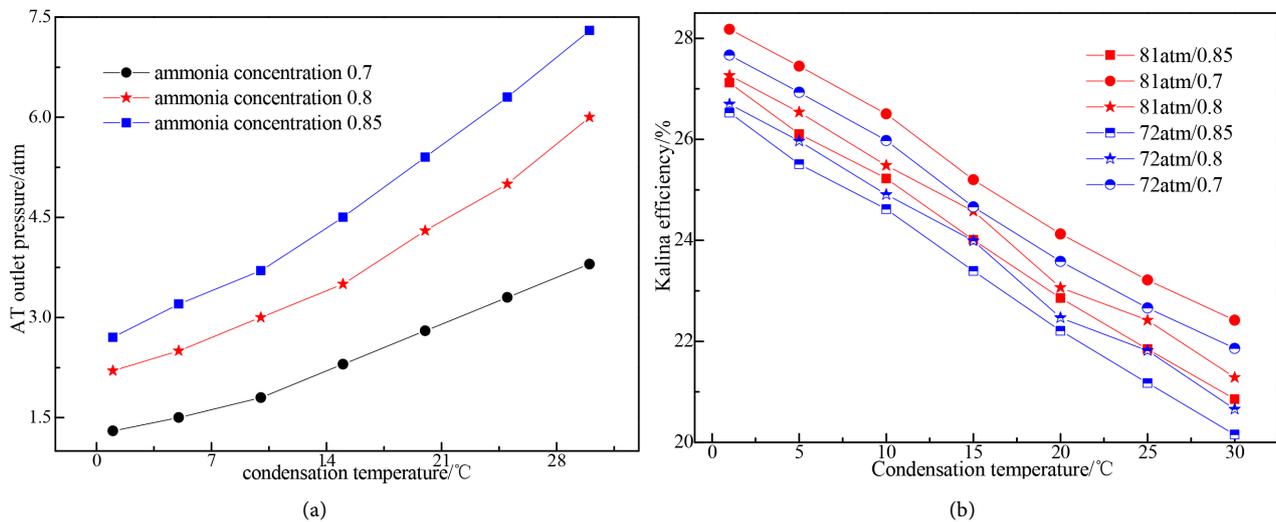
Figure 10. Influence of condensation temperature on the performance of the system.

When doing EUD analysis for a thermodynamic process, there exists two processes respectively called "energy donor" and "energy acceptor". The x-coordinate in the EUD diagram is energy change, and the y-coordinate is energy level A, which is a dimensionless criteria, the ratio of the exergy change ΔE and energy change ΔH in the thermal process. The area between Aed and Aea curves represents the exergy destruction in the energy transfer process.

4.7.1. EUD of Heat Exchange Processes

Figure 11(a) and Figure 11(b) illustrate the exergy-utilization diagram (EUD) of heat exchange processes of the proposed system and the reference system respectively. GT exhaust gas is used in two stages, at first stage is used to reheat compressed air, second is used to drive Kalina and Rankine cycle.

As can be seen from the horizontal of Figure 11(a), in Kalina cycle, the enthalpy of preheating stage is 281.97 kW, the enthalpy of ammonia generator stage is 803.31 kW. The energy level of exhaust gas acts as the energy donor, the heating process of compressed air acts as the energy acceptor. It's temperature is from 635.9°C to 805.5°C and Aed from 0.53 to 0.63. From the shaded area we can also see that the exergy losses of preheating stage and ammonia generator stage are 19.43 kW, 93.24 kW respectively. From Figure 11(b) we can see that in Rankine cycle, the enthalpy differences of preheating stage and ammonia generator stage are 281.97 kW, 792.26 kW respectively, and the corresponding exergy losses of preheating stage and ammonia generator stage are 19.43 kW, 111.9 kW respectively.

4.7.2. EUD of Power Blocks

Figure 12 illustrates the energy-utilization diagram or the power blocks in the proposed system. In the power process, GT and AT act as "energy donor", FC and AC act as "energy acceptor". The power output of the AC、FC、GT and AT are indicated by the widths of $A_{ea,AC}$ $A_{ea,FC}$ $A_{ed,GT}$ and $A_{ed,AT}$, respectively. As can
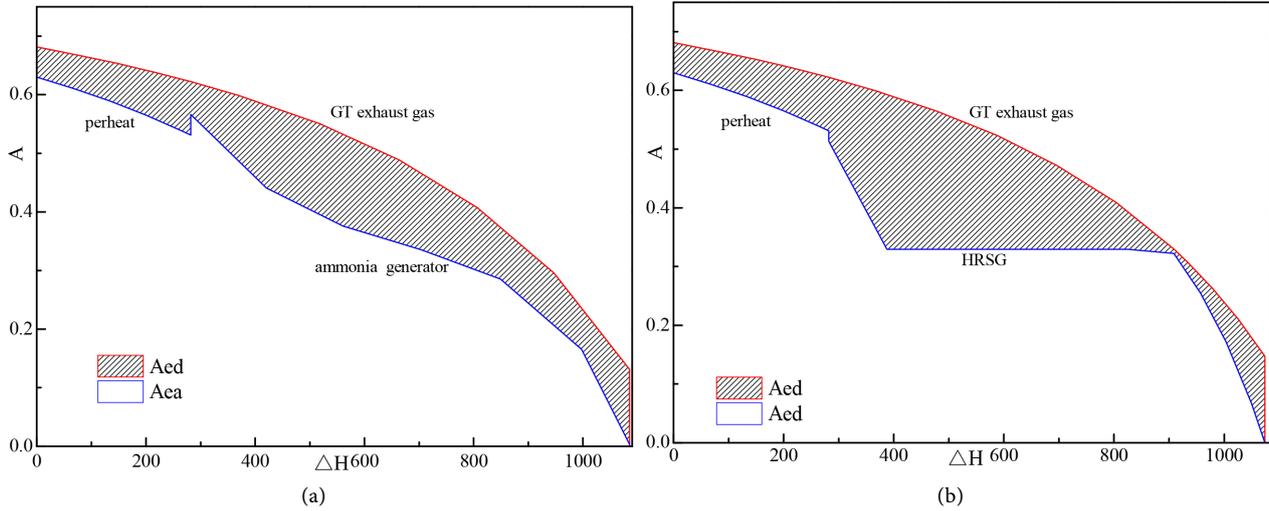
Figure 11. Energy-utilization diagram (EUD) of heat exchange processes.
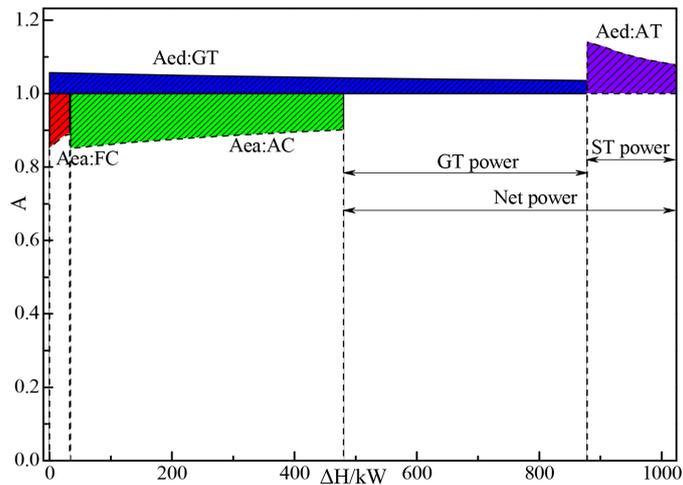
Figure 12. Energy-utilization diagram (EUD) of the power blocks.

be seen from the horizontal of **Figure 12**, the enthalpy difference of FC is 32.7 kW, the enthalpy difference of AC is 447.1 kW. The enthalpy difference of GT is 875.4 kW. The power of GT is represented by the width of the curve. From the shaded area we can also see the exergy loss of FC is 19.43 kW, AC exergy loss is 403.33 kW, GT exergy loss is 955.26 kW.

5. Conclusions

The SOFC-GT-Kalina integrated system is put forward in this paper. By energetic and exergetic performance analysis, the following conclusions can be drawn:

1) By comparison, under the given condition, electrical and exergy efficiency of the proposed system are 74.41% and 71.93%, while those of the reference system are 74.45% and 69.07%, proving the superiority of Kalina cycle for waste heat recovery.

2) The largest exergy destruction occurs in the SOFC, followed by the after-burner, ammonia steam generator and GT. By using Kalina cycle for fully using of waste heat, the exergy destruction of exhaust gas is small.

3) There exists an optimal SOFC current density at 350 mA/cm^2. Within a certain range by increasing compression ratio, air flow is conducive to system performance.

4) When other conditions remain unchanged, increasing the ammonia flow can increase the exergy destruction of ammonia generator; it has little effect on ammonia steam turbine exergy destruction.

5) With the increase of ammonia concentration, the condensation temperature should be decreased in order to achieve higher thermal efficiency. In addition, when the AT inlet pressure keeps constant, the thermal efficiency decrease with the condensation temperature.

Acknowledgements

References

[1] Zhao, Y., Xia, C., Jiao, L., *et al.* (2013) Recent Progress in Solid Oxide Fuel Cell: Lowering Temperature and Utilizing Non-Hydrogen Fuels. *International Journal Hydrogen Energy*, **38**, 498-517. https://doi.org/10.1016/j.ijhydene.2013.07.077

[2] Komatsu, Y., Kimijima, S. and Szmyd, J.S. (2010) Performance Analysis for the Part-Load Operation of a Solid Oxide Fuel Cell-Micro Gas Turbine Hybrid System. *Energy*, **35**, 2-8. https://doi.org/10.1016/j.energy.2009.06.035

[3] Bang-Moller, C., Rokni, M., Elmegaard, B., *et al.* (2013) Decentralized Combined Heat and Power Production by Two-Stage Biomass Gasification and Solid Oxide Fuel Cells. *Energy*, **58**, 27-37.

[4] Akkaya, A.V., Sahinb, B. and Erdem, H.H. (2008) An Analysis of SOFC/GT CHP System Based on Exergetic Performance Criteria. *Science Direct*, **33**, 2566-2577. https://doi.org/10.1016/j.ijhydene.2008.03.013

[5] Martinez, A.S. and Brouwer, J. (2015) Comparative Analysis of SOFC-GT Freight Locomotive Fueled by Natural Gas and Diesel with Onboard Reformation. *Applied Energy*, **148**, 421-438. https://doi.org/10.1016/j.apenergy.2015.01.093

[6] Duan, L., Huang, K. and Yang, Y. (2013) Comparison Study on Different SOFC Hybrid Systems with Zero-CO_2 Emission. *Energy*, **58**, 66-77. https://doi.org/10.1016/j.energy.2013.04.063

[7] Calise, F., Palombo, A. and Vanoli, L. (2006) Design and Partial Load Exergy Analysis of Hybrid SOFC-GT Power Plant. *Journal of Power Sources*, **158**, 225-244. https://doi.org/10.1016/j.jpowsour.2005.07.088

[8] Baniasadi, E. and Dincer, I. (2011) Energy and Exergy Analyses of a Combined Ammonia-Fed Solid Oxide Fuel Cell System for Vehicular Applications. *International Journal of Hydrogen Energy*, **36**, 11128-11136. https://doi.org/10.1016/j.ijhydene.2011.04.234

[9] El-Emam, R.S., Dincer, I. and Naterer, G.F. (2012) Energy and Exergy Analyses of an Integrated SOFC and Coal Gasification System. *International Journal Hydrogen*

Energy, **37**, 1689-1697. https://doi.org/10.1016/j.ijhydene.2011.09.139

[10] Ishak, F., Dincer, I. and Zamfirescu, C. (2012) Energy and Exergy Analyses of Direct Ammonia Solid Oxide Fuel Cell Integrated with Gas Turbine Power Cycle. *Journal of Power Sources*, **212**, 73-85. https://doi.org/10.1016/j.jpowsour.2012.03.083

[11] Gogoi, T.K., Sarmah, P. and Deb Nath, D. (2014) Energy and Exergy Based Performance Analyses of a Solid Oxide Fuel Cell Integrated Combined Cycle Power Plant. *Energy Conversion and Management*, **86**, 507-519. https://doi.org/10.1016/j.enconman.2014.06.006

[12] Motahar, S. and Alemrajabi, A.A. (2009) Exergy Based Performance Analysis of a Solid Oxide Fuel Cell and Steam Injected Gas Turbine Hybrid Power System. *International Journal Hydrogen Energy*, **34**, 2396-2407. https://doi.org/10.1016/j.ijhydene.2008.12.065

[13] Haseli, Y., Dincer, I. and Naterer, G.F. (2008) Thermodynamic Analysis of a Combined Gas Turbine Power System with a Solid Oxide Fuel Cell through Exergy. *Thermochimica Acta*, **480**, 1-9. https://doi.org/10.1016/j.tca.2008.09.007

[14] Rokni, M. (2014) Thermodynamic and Thermos Economic Analysis of a System with Biomass Gasification, Solid Oxide Fuel Cell (SOFC) and Stirling Engine. *Energy*, **76**, 19-31. https://doi.org/10.1016/j.energy.2014.01.106

[15] Mehrpooyaab, M. and Sharifzadeh, M.M.M. (2017) Conceptual and Basic Design of a Novel Integrated Cogeneration Power Plant Energy System. *Energy*, **127**, 516-533. https://doi.org/10.1016/j.energy.2017.03.127

[16] Choudhary, T. and Sanjay (2017) Thermodynamic Assessment of SOFC-ICGT Hybrid Cycle: Energy Analysis and Entropy Generation Minimization. *Energy*, **134**, 1013-1028. https://doi.org/10.1016/j.energy.2017.06.064

[17] Thallam Thattaia, A., Oldenbroeka, V., Schoenmakersb, L., Woudstraa, T. and Aravind, P.V. (2017) Towards Retrofitting Integrated Gasification Combined Cycle (IGCC) Power Plants with Solid Oxide Fuel Cells (SOFC) and CO_2 Capture—A Thermodynamic Case Study. *Applied Thermal Engineering*, **114**, 170-185. https://doi.org/10.1016/j.applthermaleng.2016.11.167

[18] Kalina, A.I. and Leibowitz, H.M. (1989) Application of the Kalina Cycle Technology Geothermal Power Generation. *Geothermal Resources Council Transactions*, **13**, 5-11.

[19] Chen, X. (1995) The Introduction of a New Kind of Thermodynamic Cycle—Kalina Cycle. *Shanghai Electric Power*, **8**, 8-10.

[20] Wang, J., Wang, J. and Dai, Y. (2008) Application of Kalina Cycle in the Low-Temperature Waste Heat Utilization. *Turbine Technology*, **50**, 207-210.

[21] Lolos, P.A. and Rogdakis, E.D. (2009) A Kalina Power Cycle Driven by Renewable Energy Sources. *Energy*, **34**, 457-464. https://doi.org/10.1016/j.energy.2008.12.011

[22] Sun, F., Ikegami, Y. and Jia, B. (2012) A Study on Kalina Solar System with an Auxiliary Super Heater. *Renewable Energy*, **4**, 210-219. https://doi.org/10.1016/j.renene.2011.10.026

[23] Zare, V. and Mahmoudi, S.M.S. (2015) A Thermodynamic Comparison between Organic Rankine and Kalina Cycles for Waste Heat Recovery from the Gas Turbine-Modular Helium Reactor. *Energy*, **79**, 398-406. https://doi.org/10.1016/j.energy.2014.11.026

[24] Zhang, X., He, M. and Zhang, Y. (2012) A Review of Research on the Kalina Cycle. *Renewable & Sustainable Energy Reviews*, **16**, 5309-5318. https://doi.org/10.1016/j.rser.2012.05.040

[25] Yue, C., Han, D. and Pu, W. (2015) Comparative Analysis of a Bottoming Transcritical ORC and a Kalina Cycle for Engine Exhaust Heat Recovery. *Energy Conversion and Management*, **89**, 764-774.
https://doi.org/10.1016/j.enconman.2014.10.029

[26] Fu, W., Zhu, J. and Li, T. (2013) Comparison of a Kalina Cycle Based Cascade Utilization System with an Existing Organic Rankine Cycle Based Geothermal Power System in an Oilfield. *Applied Thermal Engineering*, **58**, 224-233.
https://doi.org/10.1016/j.applthermaleng.2013.04.012

[27] Lv, C.R. and Yan, J.Y. (1991) The Research and Development of Kalina Cycle and an Analysis of Its Efficiency Enhancement Potentiality. *Power Engineering*, **6**, 1-7.

[28] Zhang, Y., He, M.G. and Jia, Z. (2005) First Law Based Thermodynamic Analysis of Kalian Cycle. *Power Engineering*, **25**, 708-712.

[29] Singh, O.K. and Kaushik, S.C. (2013) Energy and Exergy Analysis and Optimization of Kalina Cycle Coupled with a Coal Fired Steam Power Plant. *Applied Thermal Engineering*, **51**, 787-800. https://doi.org/10.1016/j.applthermaleng.2012.10.006

[30] Sun, F., Zhou, W. and Ikegami, Y. (2014) Energy-Exergy Analysis and Optimization of the Solar-Boosted Kalina Cycle System 11 (KCS-11). *Renewable Energy*, **66**, 268-279. https://doi.org/10.1016/j.renene.2013.12.015

[31] Arslan, O. (2010) Exergoeconomic Evaluation of Electricity Generation by the Medium Temperature Geothermal Resources, using a Kalina Cycle: Simav Case Study. *International Journal of Thermal Sciences*, **49**, 1866-1873.
https://doi.org/10.1016/j.ijthermalsci.2010.05.009

[32] Di Pippo, R. (2004) Second Law Assessment of Binary Plants Generating Power from Low-Temperature Geothermal Fluids. *Geothermics*, **33**, 565-586.
https://doi.org/10.1016/j.geothermics.2003.10.003

[33] Bombarda, P., Invernizzi, C.M. and Pietra, C. (2010) Heat Recovery from Diesel Engines: A Thermodynamic Comparison between Kalina and ORC Cycles. *Applied Thermal Engineering*, **30**, 212-219.
https://doi.org/10.1016/j.applthermaleng.2009.08.006

[34] Fu, W.C., Zhu, J.L., Li, T.L., *et al*. (2013) Comparison of a Kalina Cycle Based Cascade Utilization System with an Existing Organic Rankine Cycle Based Geothermal Power System in an Oilfield. *Applied Thermal Engineering*, **58**, 224-233.
https://doi.org/10.1016/j.applthermaleng.2013.04.012

[35] An, L., Zhang, J. and Ma, H. (2008) Solid Oxide Fuel Cell-Gas Turbine Hybrid Power System. *Renewable Energy Resources*, **26**, 62-67.

[36] Campanari, S. (2001) Thermodynamic Model and Parametric Analysis of a Tubular SOFC Module. *Journal of Power Sources*, **92**, 26-24.

Nomenclature

I: Current of the *SOFC* (A)

F: Faraday's constant (96,485.3 C/mol)

p: *SOFC* operating pressure (bar)

pref: Reference pressure (1 bar)

T: *SOFC* operating temperature (˚C)

T_{ref}: Reference pressure (1000˚C)

P_{H_2} : Partial pressures for hydrogen (bar)

P_{H_2O} : Partial pressures for water vapor (bar)

P_{O_2} : Average oxygen partial pressure in cathode (bar)

V_{SOFC}: *SOFC* voltage (V)

V_{ref}: reference voltage

WDC: *SOFC* DC power

WAC: *SOFC* AC power

η_{SOFC} : *SOFC* electrical efficiency

η : Electrical efficiency

W: Electrical power

η_{ex} : Exergy efficiency

Ex_{gain}: Exergy benefits

Ex_{pay}: Exergy cost

Ex_L: Exergy loss

EUD: Energy-utilization diagram

A: Energy level

Variable

q_{CH_4} : Mole flow rate (mol/s)

A_{cell}: The active area of one single cell (m²)

N_{cell}: The total numbers of the cell

m_i: Fuel flow rate (kg/s)

LHVf: Low heat value of fuel (kJ/kg)

x: Ammonia mass concentration (%)

ΔV_p : Influence of operating pressure on the voltage (mV)

ΔV_T : Influence of operating temperature on the voltage (mV)

ΔE : Exergy change (kJ/mol)

ΔH : Enthalpy change (kJ/mol)

Abbreviation

KCS: Kalina cycle system

ICE: Internal combustion engine

SOFC: Solid oxide fuel cell

RC: Rankine cycle

ST: Steam turbine

GT: Gas turbine

HE: Heat exchanger

AT: Ammonia steam turbine

pro-s: The proposed system

ref-s: The reference system

HRSG: Heat recovery steam generator

HP: High-pressure pump

LP: Low-pressure pump

CW: Cooling water

HE: heat exchanger

AB: After-burner

an: *SOFC* anode

ca: *SOFC* cathode

AC: Air compressor

FC: Fuel compressor

temp: Temperature

TIT: Turbine inlet temperature